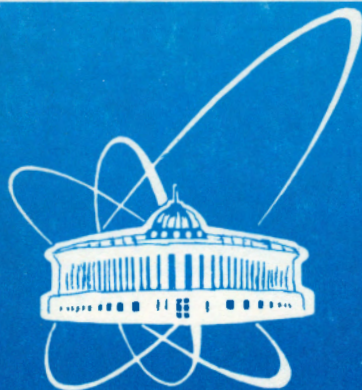


98-266



СООБЩЕНИЯ
ОБЪЕДИНЕННОГО
ИНСТИТУТА
ЯДЕРНЫХ
ИССЛЕДОВАНИЙ

Дубна

98-266

E7-98-266

H.Sakurai¹, S.M.Lukyanov, M.Notani¹, N.Aoi², D.Beaumel^{1,4},
N.Fukuda², M.Hirai², E.Ideguchi¹, N.Imai², M.Ishihara^{1,4},
H.Iwasaki², T.Kubo¹, K.Kusaka¹, H.Kumagai¹, T.Nakamura²,
H.Ogawa³, Yu.E.Penionzhkevich, T.Teranishi¹,
Y.X.Watanabe², K.Yoneda², A.Yoshida¹

EVIDENCE FOR PARTICLE STABILITY OF ^{31}F
AND PARTICLE INSTABILITY OF ^{25}N AND ^{28}O .

¹RIKEN (The Institute of Physical and Chemical Research), Saitama, Japan

²Department of Physics, University of Tokyo, Japan

³Department of Applied Physics, Tokyo Institute of Technology, Japan

⁴Institute de Physique Nucléaire, Orsay Cedex, France.

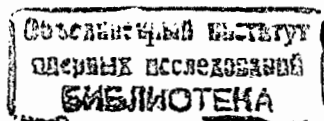
1998

The experimental determination of the neutron drip line is essential for the understanding of the nuclear stability for extreme isospin asymmetry. It was once suggested [1] that the neutron drip line appears to be experimentally mapped out up to the $Z=10$ isotopes, in comparing the observed heaviest isotopes with mass formula predictions [2]. Since then, however, our knowledge has been considerably extended concerning the stability of extremely neutron-rich isotopes, and renewed efforts to search for new isotopes beyond the presently adopted drip line have been encouraged.

The recent discovery of the particle stability of ^{31}Ne [3], in contrast to most of mass predictions, has motivated us to re-examine the location of the fluorine drip line. ^{31}Ne is located at the deformation region centered at $Z\sim 11$ and $N\sim 20$, the so-called 'island of inversion' region. A particular feature in this region is the tendency towards prolate deformation in spite of the effect of spherical stability due to the magicity of the neutron number of 20 [4, 5, 6, 7, 8, 9]. As a matter of fact, a large $B(E2; 0^+ \rightarrow 2^+)$ value was observed for the $N=20$ nucleus ^{32}Mg [10], supporting the possibility of considerable deformation. It is also argued that the deformation may account for the enhanced binding energies manifested by some of the known nuclei in this region [11]. Thus, the extra stability of ^{31}Ne may be due to the deformation effect. The presently observed heaviest fluorine isotope, ^{29}F [12] with $N=20$, is in harmony with various mass predictions [2, 6, 9, 13] with or without deformation effects included. It should be noted, however, that the particle stability of ^{31}F with $N=22$ has been predicted by some theoretical studies including deformation effects [9, 13]. Interestingly, these theories also predict the particle stability of ^{31}Ne , in agreement with the experimental finding.

Toward a lower Z along $N=20$, the question of the possible stability of the double magic nucleus, ^{28}O , has recently attracted much attention, even though the particle instability of $^{25,26}\text{O}$ beyond ^{24}O has been clearly shown by two experiments [14, 15]. The expectation for ^{28}O to be stable stems from an enhanced stability anticipated from the double magicity or the deformation. The stability of ^{28}O has been discussed in several theoretical papers [2, 6, 13, 16, 17, 18], which however yielded conflicting results. Recently, an attempt to search for ^{28}O has been made by using a ^{36}S beam [19]. In that work, no events of ^{28}O were observed, and the particle instability of ^{28}O was concluded from a comparison with the larger estimated yield for particle stable ^{28}O . The yield estimate was made by means of an extrapolation method using the results of heavier isotones of $N=20$. Such extrapolation may, however, involve some ambiguities since the Z, A dependence of the production cross sections is not well understood theoretically. In order to reduce possible uncertainty, use of an interpolation method, which was once applied for the first evidence for the instability of ^{26}O [14], should be desirable.

This Letter presents the results of an attempt to determine the neutron drip line for the nitrogen, oxygen and fluorine isotopes over the region extending up to $N\leq 22$. An experimental difficulty in the search for new isotopes beyond the heaviest observed nuclei is the low production rates. However, these difficulties have been considerably reduced by the combination of a high-energy, high-intensity ^{40}Ar beam with the RIKEN Projectile Fragment Separator (RIPS) [20]. The ^{40}Ar projectile is inferior to ^{36}S in terms of the production cross sections for very neutron-rich fragments with $N\leq 20$. Compared with ^{36}S ,



however, ^{40}Ar has a wider dynamic range for production by covering a region ranging up to $N=22$. Moreover, the ^{40}Ar beam can be obtained at a higher energy of 94.1A MeV and with a high intensity of about 45 pA. The use of RIPS is also helpful for increasing the reaction yield by virtue of its large momentum acceptance (6%), solid angle (5msr), and sizable maximum magnetic rigidity of 5.76 Tm. With all of these factors combined, an effective luminosity as high as $10^{32} \text{ cm}^{-2} \text{ s}^{-1}$ has been achieved.

The ^{40}Ar beam accelerated at the AVF and RIKEN Ring Cyclotron reacted with a 690 mg/cm² thick ^{nat}Ta target. The target thickness was chosen to maximize the secondary beam intensities based on a semiempirical yield estimation by the INTENSITY code [21]. The primary beam current was monitored by an array of plastic detectors located near the production target.

The reaction fragments were collected and analyzed by RIPS operated in an achromatic mode and at the maximum values of momentum acceptance and solid angle. The magnetic rigidity of the first half of RIPS was set at 4.53 Tm in order to optimize the yield of the ^{28}O isotope. To reduce the relative rates of light isotopes, such as those of $Z=1-3$, an aluminum wedge with a mean thickness of 226.2 mg/cm² was used at the momentum dispersive focal plane (F1). The magnetic rigidity of the second part of the RIPS spectrometer was thereby adjusted to 4.42 Tm.

Particle identification was performed by a standard method on the basis of energy loss (ΔE), total kinetic energy (TKE), time-of-flight (TOF) and magnetic rigidity ($B\rho$) measured for each fragment [3].

The positions of the fragments at the momentum dispersive focal plane (F1) were recorded using a parallel plate avalanche counter (PPAC) in order to determine the $B\rho$ values. The sensitive area of this PPAC was 15cm(H) \times 10cm(V), which covered a full rigidity acceptance of 6%. The charge division method was applied for position reading. The PPAC was equipped with four independent cathodes stripped horizontally. The multifold cathode served to reject spurious position information due to δ -rays, and to reach a high level of detection efficiency by imposing a condition of more than two hits being observed out of the four cathodes. The typical efficiency for a $Z=4$ particle was over 95%.

The fragmentation products reached the final focal point (F3) of the RIPS spectrometer, where a plastic scintillation counter (F3-PI) with a thickness of 1 mm and a telescope consisting of 6 lithium-drift silicon detectors (SSD) were installed. A plastic veto counter with a thickness of 1 mm was located behind the SSD telescope. The thicknesses of the silicon detectors were 1.1, 1.1, 3.1, 2.9, 4.0 and 4.3 mm, respectively. The thicknesses of the detectors were chosen so as to stop the fragments of interest in the fifth detector. The active area of the first four detectors was 48 mm \times 48 mm and the last two had a sensitive diameter of about 35 mm. The time-of-flight (TOF) of each fragment was determined from the F3-PI timing and the RF signal of the cyclotron. Typical flight times were about 250 ns. Each SSD detector provided independent energy-loss values (ΔE), while the whole telescope provided the total kinetic energy (TKE). The veto counter was used to reject pile-up events due to light fragments.

The atomic number (Z) of a fragment was determined from the ΔE at the first four detectors and from the TOF information. The accuracy in the Z determination was about

0.8% for the nitrogen isotopes. The mass-to-charge ratio (A/Q) was obtained with an accuracy of 0.5% for the same isotopes. The fragment charge (Q) was obtained from the combination of TKE, $B\rho$ and TOF. For the final analysis, we employed fully stripped fragments by imposing a condition that the relation $|Z - Q|/Z \leq 6.5\%$ should hold.

At the first achromatic focal plane (F2) the horizontal aperture was tuned to be ± 25 mm by the slits to match with the area of the SSD telescope. At this plane horizontal and vertical position distributions of the nuclei of interest were measured by another charge-divisional PPAC with two cathodes. Those position spectra were used to diagnose the profile of the secondary beam. The horizontal position distributions of the isotopes transmitted to the F2 are given in Fig.1. The arrows in this figure show the position centroids estimated for the isotopes of interest by an energy loss calculation. We found that the centroids experimentally detected for the ^{22}C and ^{29}F isotopes were in agreement with the calculated results within about 1 mm. This consistency assured that the RIPS tuning was optimal for the neutron-rich N-F isotopes. Note that this estimation also predicts that the events for the $^{24,25}\text{N}$, $^{26-28}\text{O}$ and ^{31}F isotopes are to be safely located in the middle of F2, as indicated by the vertical arrows in Fig.1.

Figure 2 shows a two-dimensional scatter plot, A/Z versus Z , obtained from the data accumulated for four days with a mean primary beam intensity of 45 pA. The number of events obtained was 4387, 7072 and 905 for the isotopes ^{19}B , ^{23}N and ^{22}C , respectively. A new isotope ^{31}F (8 events) was observed for the first time. In addition to the identification by A/Z and Z , the F2 position distribution of the ^{31}F isotope, as demonstrated in Fig.1 (solid line histogram), was in good agreement with the calculated position. The production cross section of ^{31}F was then obtained to be about 0.15 ± 0.06 pb. The absence of events corresponding to the $^{25,26,27,28}\text{O}$ isotopes as well as $^{24,25}\text{N}$ and ^{30}F is clearly confirmed. For instance, in the case of the particle stability of ^{28}O or ^{25}N , the associate events are expected to appear inside the ellipses in Fig.2, while no events were found in those domains.

The non-observation of an isotope does not necessarily prove its unbound character. To achieve more definite evidence, we plotted the observed yields versus Z for the nuclei with $N=2Z+4$, as shown in Fig.3. A smooth and monotonous decrease of the experimental yields is observed through the isotopes. The solid line in Fig.3 represents the yields expected by INTENSITY, which includes the EPAX parameterization for the production cross sections [22]. We modified a parameter U in EPAX from the standard value of 1.5 to 1.6 to best reproduce the yields for the very neutron-rich fragments. Such a modification was also made in Refs. [19, 23]. The calculated yields are in good agreement with the observed yields over the whole range, connecting smoothly the results of ^{22}C and ^{31}F . The yields of ^{25}N and ^{28}O , which lie between ^{22}C and ^{31}F , can therefore be estimated with fair reliability by the interpolation method. We then obtain yield estimates of 240 and 37 events, respectively, for ^{25}N and ^{28}O . The interpolation method has been also applied to the data of $N=2Z+2$ and $N=2Z+4$ to estimate the yields of the $N=2Z+3$ nuclides. The fact that the experimental results of no events distinctly deviate from these estimated yields provides strong evidence for the particle instability of $^{24,25}\text{N}$, $^{27,28}\text{O}$ and ^{30}F .

In an earlier work [19], the expected yield of ^{28}O was estimated from an extrapolation procedure on the basis of the measured yields for the $N=20$ isotones. However, such an

extrapolation may require a reliable theoretical guidance for the production cross sections of fragments. In contrast, the present interpolation method is essentially free of theories on the production yield. Also note that the upper limit for the ^{28}O cross section set by the present data is about 0.02 pb, which is roughly one order of magnitude lower than that given in Ref. [19]. These arguments strengthen the conclusion that ^{28}O is indeed particle instable.

We have confirmed that the heaviest nitrogen and oxygen isotopes are ^{23}N and ^{24}O with the same neutron number, $N=16$, while the heaviest isotope of fluorine has been extended up to ^{31}F with $N=22$. It is remarkable that six additional neutrons can be bound by moving from oxygen to fluorine, where Z differs only by one. Concerning the instability of $^{24,25}\text{N}$, mass formula predictions [2] are in agreement with our results. On the other hand, the locations of the drip line for oxygen and fluorine are hardly predicted by the mass formulas, most of which favor ^{26}O and ^{29}F for the heaviest isotopes.

The sudden change in stability from oxygen to fluorine indicates an extra push of stability for the very neutron-rich fluorine isotopes. Among the mass formulas, only the finite-range droplet model (FRDM) [13] predicts the stability of ^{31}F . The FRDM includes nuclear deformation effects for both the macroscopic and microscopic parts. It is interesting to note that the same FRDM predicts the particle stability of ^{31}Ne , in agreement with the result of a recent experiment [3].

The stability of ^{31}F can be also treated theoretically in terms of a shell model. There are two such calculations: one by Poves *et al.* (PR) [9] and another by Warburton *et al.* (WBB) [6]. The PR model demands strong configuration mixing between the sd and fp shells to explain the known ground-state spins of $^{29,31}\text{Na}$, while the WBB model calculation resulted in a smaller mixing between these two shells, failing to reproduce the ground state spins. These two models also disagree in predicting the particle stability of ^{31}F , the PR predicting stability and the WBB instability. This discrepancy appears to arise from a difference in the degree of mixing between the two major shells. Here again, the importance of a deformation effect is suggested, since strong mixing, as considered in the PR model, may be tied with the tendency toward deformation.

In contrast, the instability of ^{28}O indicates the unimportance of the deformation effects. In another work with the PR model [16], two different sets of valence spaces were employed for binding energy calculations: a conventional configuration up to the sd shell and a wide configuration including the fp shell. The former case led to the instability of ^{28}O , but the latter to stability. A calculation by the WBB model also predicted ^{28}O to be instable. These results indicate that the trend is opposite to the case of ^{31}F : two models with weaker mixing between the two shells are consistent with the experimental findings, while the other with stronger mixing fails to reproduce it. It is thus probable that the distinct difference in the particle stability is related to a sudden onset of deformation for the fluorine isotopes.

In summary, the new neutron-rich isotope ^{31}F was observed for the first time using the RIPS spectrometer with the reaction $^{40}\text{Ar} + ^{nat}\text{Ta}$ at 94.1A MeV. Besides, clear evidence of the particle instability of $^{24,25}\text{N}$, $^{27,28}\text{O}$ and ^{30}F was obtained on the basis of an interpolation of the experimental yields. These results serve to re-define the map of the particle stability and neutron drip line up to fluorine isotopes.

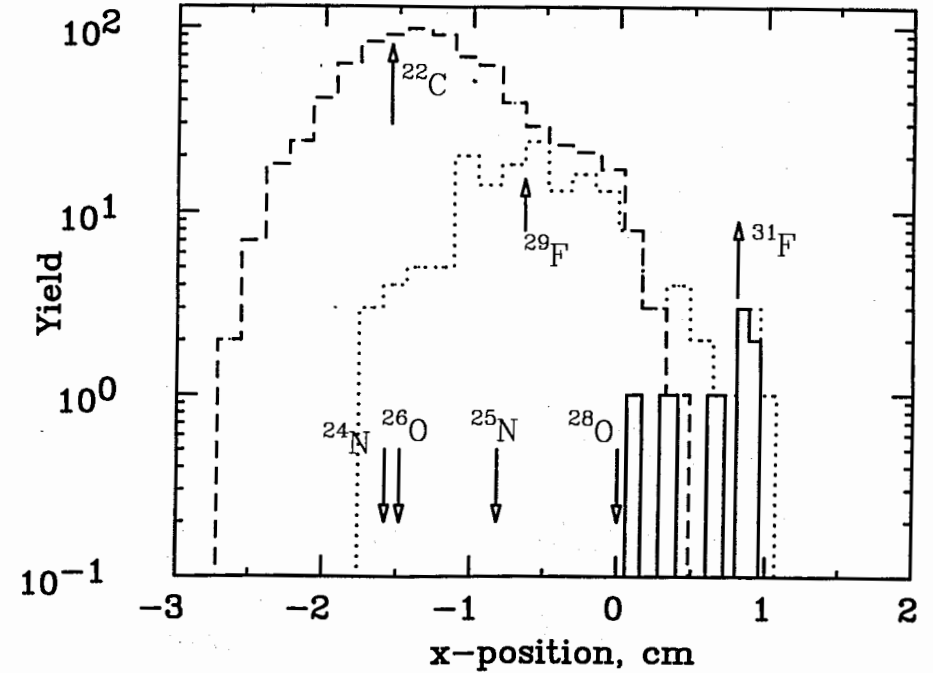


FIG. 1. Experimental distributions of the horizontal positions for isotopes transmitted to the first focal plane (F2) of the RIPS spectrometer. The centroids experimentally detected for the ^{22}C (dashed histogram) and ^{29}F (dotted histogram) isotopes were in agreement with the calculated values (up arrows) obtained by an energy loss calculation. The position distribution of ^{31}F isotope (solid line histogram) was also in accord with the calculation. The expected events for $^{24,25}\text{N}$ and $^{26,28}\text{O}$ could be centered at the middle of F2, and their expected center positions are shown by the down arrows.

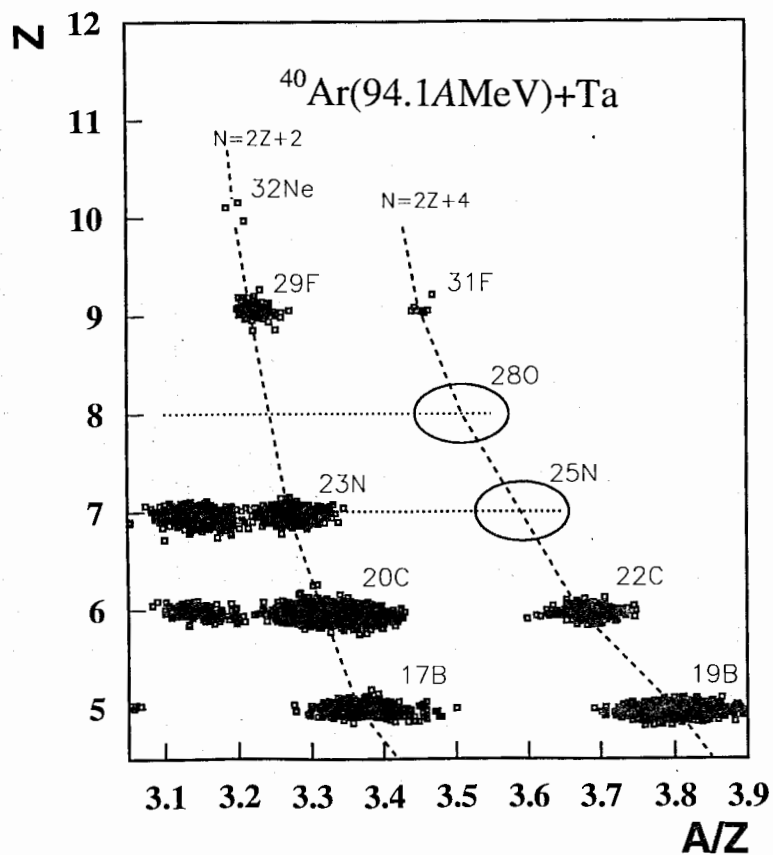


FIG. 2. Two-dimensional A/Z versus Z plot, which was obtained in the reaction of a 94.1 MeV ^{40}Ar beam on a 690 mg/cm² tantalum target during a 4-day run. A new isotope ^{31}F is clearly visible (8 events). No events associated with ^{25}N and ^{28}O as well as ^{24}N , $^{25,26,27}\text{O}$ and ^{30}F were obtained. In the case of the particle stability of ^{28}O or ^{25}N , the associate events are expected to appear inside the ellipses. The dashed lines are drawn guides to the eye for the isotopes with the same neutron numbers, $N=2Z+2$ and $N=2Z+4$.

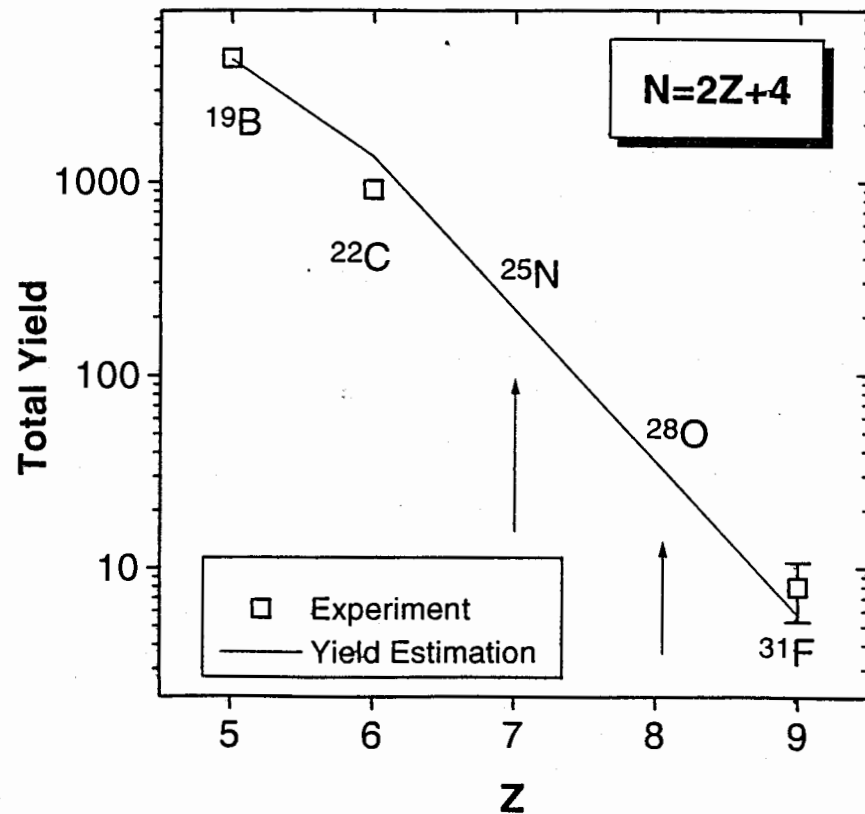


FIG. 3. Isotopic production for nuclei with the neutron number $N=2Z+4$. The solid curve presents the expected yields according to the INTENSITY using the modified EPAX parameterization. The expected yields for ^{28}O and ^{25}N are indicated by arrows.

Our sincere gratitude is extended to the staff members of the RIKEN ring cyclotron for their operation of the ECR and accelerator. One of the authors (S.L.) gives thanks for support from RIKEN. The authors (S.L. and Y.P.) acknowledge partial support by the Russian Foundation for Fundamental Research (RFFI) under grand No. 96-02-17381a.

REFERENCES

- C. Detraz and D.J. Vieira, *Annu. Rev. Nucl. Part. Sci.* 39, 407 (1989); A.C. Mueller and B.M. Sherrill, *Annu. Rev. Nucl. Part. Sci.* 43, 529 (1993).
- 1986–1987 *Atomic Mass Predictions*, edited by P.E. Haustein [*At. Data Nucl. Data Tables* 39, 185 (1988)].
- H. Sakurai *et al.*, *Phys. Rev. C* 54, R2802 (1996).
- X. Campi *et al.*, *Nucl. Phys.* A251, 193 (1975).
- R. Nayak and L. Satpathy, *Nucl. Phys.* A304, 64 (1978).
- E.K. Warburton, J.A. Becker and B.A. Brown, *Phys. Rev. C* 41, 1147 (1990).
- S.K. Patra and C.K. Praharaj, *Phys. Lett. B* 273, 13 (1991).
- M. Fukunishi, T. Otsuka and T. Sebe, *Phys. Lett. B* 292, 279 (1992).
- A. Poves and J. Retamosa, *Nucl. Phys.* A571, 221 (1994).
- T. Motobayashi *et al.*, *Phys. Lett. B* 346, 9 (1996).
- N.A. Orr *et al.*, *Phys. Lett. B* 258, 29 (1991); X.G. Zhou *et al.*, *Phys. Lett. B* 260, 285 (1991).
- D. Guillemaud-Mueller *et al.*, *Z. Phys. A* 332, 189 (1989).
- P. Möller *et al.*, *At. Data Nucl. Data Tables* 39, 185 (1995).
- D. Guillemaud-Mueller *et al.*, *Phys. Rev. C* 41, 937 (1990).
- M. Fauerbach *et al.*, *Phys. Rev. C* 53, 647 (1996).
- A. Poves *et al.*, *Z. Phys. A* 347, 227 (1994).
- Z. Ren *et al.*, *Phys. Rev. C* 52, R20 (1995).
- A.T. Kruppa *et al.*, *Phys. Rev. Lett.* 79, 2217 (1997).
- O. Tarasov *et al.*, *Phys. Lett. B* 409, 64 (1997).
- T. Kubo *et al.*, *Nucl. Instrum. Methods B* 70, 309 (1992).
- J.A. Winger, B.M. Sherrill and D.J. Morrissey, *Nucl. Instrum. Methods B* 70, 380 (1992).
- K. Sümmerer *et al.*, *Phys. Rev. C* 42, 2546 (1990).
- R. Pfaff *et al.*, *Phys. Rev. C* 53, 1753 (1996).

Received by Publishing Department
on December 28, 1998.

Сакурай Х. и др.

E7-98-266

Ядерная стабильность ^{31}F и нестабильность ядер ^{25}N и ^{28}O

Исследования стабильности нейтроноизбыточных ядер предприняты в реакции фрагментации ионов ^{40}Ar с энергией 94,1 МэВ · А на сепараторе RIPS (RIKEN, Япония). Впервые экспериментально обнаружена ядерная стабильность ядра ^{31}F . Приводятся экспериментальные данные, свидетельствующие о нестабильности следующих ядер: $^{24,25}\text{N}$, $^{27,28}\text{O}$ и ^{30}F . Полученные экспериментальные данные анализируются на основе влияния деформации на стабильность ядер в этой области.

Работа выполнена в Лаборатории ядерных реакций им. Г.Н.Флерова ОИЯИ.

Сообщение Объединенного института ядерных исследований. Дубна, 1998

Sakurai H. et al.

E7-98-266

Evidence for Particle Stability of ^{31}F and Particle Instability of ^{25}N and ^{28}O

Neutron drip line determinations up to fluorine have been performed by the projectile fragmentation of a 94.1 A · MeV ^{40}Ar beam using the fragment separator RIPS at RIKEN (Japan). A new neutron-rich isotope ^{31}F has been observed for the first time, while clear evidence for the particle instability of $^{24,25}\text{N}$, $^{27,28}\text{O}$ and ^{30}F has been obtained. The sudden change in stability from oxygen to fluorine may demonstrate the onset of a deformation phenomenon for neutron-rich fluorine isotopes.

The investigation has been performed at the Fleroy Laboratory of Nuclear Reactions, JINR.

Communication of the Joint Institute for Nuclear Research. Dubna, 1998